*International Journal of Applied Engineering and Technology ISSN: 2277-212X*
*An Open Access, Online International Journal Available at http://www.cibtech.org/jet.htm*
*2022, Vol.12, pp.12-22/Edward*
***Research Article***

# THE CHARACTERISTICS AND HYDRODYNAMICS OF THE RIVER CONFLUENCES

***LUO Ching-Ruey (Edward)**
*Department of Civil Engineering, National Chi-Nan University, Nantou, Taiwan*
**Author for Correspondence: edward.luo@msa.hinet.net*

## ABSTRACT
Diffusion and differential advection are identified as the main processes governing mixing and sediment transferring in natural streams. The interaction between these two processes is shown to enhance the rates of spreading in the longitudinal direction and this effect is termed dispersion. It is expressed that in steady-state situations, such as those resulting from continuous releases at constant rate, analytical predictions are possible using a transformation that substitutes distance across the channel by the corresponding fraction of discharge. However, transient mixing is a relatively complex process and requires use of numerical techniques of computation. Engineering application is shown to depend on knowledge of the transverse mixing coefficient with the combination effects of turbulent diffusion and dispersion due to secondary currents. In natural streams, the additional effect of transverse dispersion due to helical motions at river bends and river non-uniformity is more important. In this paper the concepts of vectors, the 1D flow solutions for both confluence and diffluence, and the 2D&3D turbulent phenomena are presented and discussed.

***Keywords:*** *Diffusion; Advection; Dispersion; Confluence; Diffluence; Secondary currents; Turbulence*

## INTRODUCTION
River confluences are important nodes in both dendritic and braided river networks. An understanding of the flow structures generated at these sites is important for predictions of scour and fill and subsequent channel change and deposition. The fluid dynamics of channel junctions is also vital for assessing mixing of the two tributaries, which affects dispersion of solutes and suspended sediment, and hence, pollutants.
Diffusion can be defined as the process by which a substance suspended or dissolved in a fluid is transferred from regions of high concentration to regions of low concentration by random motions within the fluid. Such random motions can be either molecular or turbulent and close examination of their effects reveals the nature of diffusion as well as the pertinent quantitative law, known as "Fick's Law":

$F_n$=-$\varepsilon_n$($\partial$C/ $\partial$n)……(1)

in which, $F_n$is diffusive flux (rate of net mass transfer per unit area) in a direction n; $\partial C/\partial n$ is the concentration gradient in the direction n; and , $\varepsilon_n$is a diffusion coefficient or "diffusivity." For molecular diffusion, $\varepsilon_n$, is a fluid property, analogous to kinematic viscosity. However, for turbulent diffusion, $\varepsilon_n$ , is a property of the flow and generally changes with position in the flow; for a given position, it generally changes with orientation. For the type of flows of interest to hydraulic engineers, which are almost invariably turbulent, molecular and turbulent diffusion occur simultaneously and thus the effective diffusivity will be the sum of the two coefficients. However, turbulent diffusion is much stronger than molecular and, for practical purposes, the latter is generally neglected. The term "advection" is used herein to denote the transport of a diffusing substance by local mean flow velocities. This process would present no particular difficulty, if the flows considered exhibited uniform velocity distributions. However, natural streams are typical cases of the so-called shear flow, characterized by significant velocity gradients in both vertical and transverse directions. Non-uniform velocity distributions cause differential advection and it is this process that further complicates mixing in natural streams.

**THEORETICAL CONSIDERATION**

In structural dynamics, it is customary to employ Lagrangian coordinates are employed customarily as the basis for numerical solution algorithms. In fluid dynamics, however, both Lagrangian and Eulerian coordinates have been used with considerable success. Because each coordinate representation has unique advantages and disadvantages depending on the characteristics of the problem to be solved.

In the case of a free fluid boundary, the time evolution of the height function is governed by a kinematic equation expressing the fact that the surface must move with the fluid,

$$\frac{\partial h}{\partial t} + u\frac{\partial h}{\partial x} = v, \qquad \text{……..(2)}$$

$$\frac{\partial F}{\partial t} + u\frac{\partial F}{\partial x} + v\frac{\partial F}{\partial y} = 0. \qquad \text{……..(3)}$$

where (u, v) are fluid velocity components in the (x, y) coordinate directions. It should be noted that Eq. (2) is Eulerian in the horizontal direction, but Lagrangian like in the vertical direction, which is more or less normal to the surface. Finite difference approximations to this equation are easily made. The height function method is directly extendable to three-dimensional situations for single-valued surfaces describable by, e.g., h =f(x, y, t). Eq. (3) states that F moves with the fluid, and is the partial differential equation analog of marker particles. In a Lagrangian mesh, Eq. (3) reduces to the statement that F remains constant in each cell.

The fluid equations to be solved are the Navier-Stokes equations,

$$\frac{\partial u}{\partial t} + u\frac{\partial u}{\partial x} + v\frac{\partial u}{\partial y} = -\frac{\partial p}{\partial x} + g_x + \nu\left[\frac{\partial^2 u}{\partial x^2} + \frac{\partial^2 u}{\partial y^2} + \xi\left(\frac{1}{x}\frac{\partial u}{\partial x} - \frac{u}{x^2}\right)\right],$$

$$\frac{\partial v}{\partial t} + u\frac{\partial v}{\partial x} + v\frac{\partial v}{\partial y} = -\frac{\partial p}{\partial y} + g_y + \nu\left[\frac{\partial^2 v}{\partial x^2} + \frac{\partial^2 v}{\partial y^2} + \frac{\xi}{x}\frac{\partial v}{\partial x}\right]. \qquad \text{……..(4)}$$

Velocity components (u, v) are in the Cartesian coordinate directions (x, y) or cylindrical coordinate directions (r, z), respectively. The choice of coordinate system is governed by the value of$\xi$, where$\xi$=0 corresponds to Cartesian and$\xi$= 1 to cylindrical geometry. Body accelerations are denoted by ($g_x$,$g_y$) and $\nu$ is the coefficient of kinematic viscosity. Fluid density has been normalized to unity. For an incompressible fluid, the momentum equations, Eqs. (4), must be supplemented with the incompressibility condition,

$$\frac{\partial u}{\partial x} + \frac{\partial v}{\partial y} + \frac{\xi u}{x} = 0. \qquad \text{……..(5)}$$

Sometimes, it is desirable to allow limited compressibility effects (e.g., acoustic waves) in which case Eq. (5) must be replaced with

$$\frac{1}{c^2}\frac{\partial p}{\partial t} + \frac{\partial u}{\partial x} + \frac{\partial v}{\partial y} + \frac{\xi u}{x} = 0, \qquad \text{……..(6)}$$

where c is the adiabatic speed of sound in the fluid (and the mean density is unity) and Eq. (6) adds more flexibility with little additional complexity.

At many, if not most, junctions of natural channels, the heights of the beds of the two confluent rivers are discordant (Kennedy, 1984). Some studies have highlighted the important morphological influence of discordant beds on the structure of flow at channel confluences (Bradbrook, *et al.*, 2001). The velocity ratio VR and depth ratio DR between the two tributaries were defined as VR = velocity in angled tributary/velocity in straight tributary and DR = depth of angled tributary/depth of straight tributary. Here,

we can see the angle of the confluence would be an important factor.The presence of a tributary step gives rise to a lateral motion of fluid from the deeper channel towards the shallower tributary, and results in distortion of the mixing layer between the two flows and fluid upwelling in the tributary channel (Best and Roy, 1991; Biron *et al.*, 1996 a,b). Such distortion has been shown in field studies to significantly enhance the mixing of the two flows (Gaudet and Roy, 1995) and widen the zone influenced by the mixing layer (Biron et al.,1993a). These effects can be of considerable importance for studies of transport, mixing and deposition of contaminated media (e.g., Axtmann *et al.*, 1997). Furthermore, to ascertain the importance of the mixing layer on the generation of Reynolds stresses and transport of sediment, the interactions between turbulent structures in the mixing interface and coherent structures within the mean field of flow must also be examined. The confluence was surveyed on the ratio of momentum flux, Mr, varied from and is defined by

$$M_r = \frac{\rho_{Ber} U_{Ber} Q_{Ber}}{\rho_{Bay} U_{Bay} Q_{Bay}} \quad \ldots\ldots(7)$$

in which $\rho$ is water density, U and Q are mean velocity and discharge, respectively, and subscripts Ber and Bay refer to the tributary and main channel, respectively. Therefore, the results illustrate a wide range of conditions where either the tributary (Mr > 1) or the main channel (Mr < 1) is dominant. To monitor stages of flow at the peak and on the falling limb of the hydrograph, the survey dates were chosen with respect to the occurrence of floods.
Turbulent kinetic energy k is defined as:

$$k = 0.5 \times \left(\overline{u'^2} + \overline{v'^2} + \overline{w'^2}\right) \quad \ldots\ldots(8)$$

Turbulent kinetic energy represents the energy extracted from the mean flow by motion of the turbulent eddies (Bradshaw, 1985) and is non-dimensionalized with respect to $U_{max}$ where $U_{max}$ is the maximal downstream velocity. Despite the changing hydraulic conditions, the spatial distribution of turbulent kinetic energy displayed a number of common characteristics. Measurements of mean and instantaneous velocity have highlighted several key characteristics of the three-dimensional field of flow at the confluence, and the zone of the downstream junction corner was characterized by low velocities without any clear recirculation motion (Bernard *et al.*, 1998).
The zone of increased values of k widened downstream. The width of this region of high turbulent kinetic energy, however, did not necessarily delimit the width of the mixing layer, but rather the limit of lateral oscillations in the position of the mixing layer. Indeed, this plane of mixing did not occupy a fixed spatial position, but underwent short term lateral fluctuations that depended on instantaneous variations of the flow field within the two streams. Because, as mixing occurs downstream, an amplification of the lateral shifts of the mixing interface exists, these oscillations were partly responsible for the downstream widening of the zone of high turbulence levels. As documented in past studies of free mixing layers, the widening of this region of high k also resulted from the downstream expansion, caused by vortex pairing and amalgamation, of turbulent structures within the mixing layer. On either side of the mixing layer in the ambient freestream, values of turbulent kinetic energy were comparable to those observed upstream from the junction in both rivers. The lateral transition from the ambient freestream to the highly turbulent mixing layer zone was characterized by sharp edges, particularly in the upstream cross-sections. The peak in turbulent kinetic energy generally occurred near the junction apex. This indicates that the generation of turbulence was greatest where mixing begins to take place and where instantaneous lateral gradients in velocity and pressure between the two streams may be expected to be highest. Turbulent kinetic energy decreased downstream because flow mixing and dissipation of turbulence can be quite rapid at times. For instance, values of k are sometimes similar to those upstream from the confluence.

*International Journal of Applied Engineering and Technology ISSN: 2277-212X*
*An Open Access, Online International Journal Available at http://www.cibtech.org/jet.htm*
*2022, Vol.12, pp.12-22/Edward*
***Research Article***

**INFLUENCE FACTORS FOR CONFLUENCE ON BOTH FLOW AND SEDIMENT TRANSPORT**

River channel confluences are rather important interfaces where intense changes in physical, mixing and sediment transport processes occur. The main flow mechanisms in confluences and the development of the shear layer formed between the two tributary flows are comprised changes in the flow discharge and channel widths of the tributaries, the influence of width and discharge ratios on the turbulent flow structure and shear layer is also evaluated. Changes in the difference between momentum ratio in the tributaries have a significant effect on the magnitude and location of flow mechanisms. Tributary flows cannot remain attached to the wall in the joint confluence and in most cases, flow separation was formed near the lateral walls. This separation zone spread in the streamwise direction in accordance with the velocity magnitude which seems to depend mainly on the momentum ratio between the tributary flows. This flow element was observed in whole vertical plans. Near the channel bed, the strength of this separation zone was higher than near the surface where flow tended to move streamwise rather than forming separation area. Flow deflection was observed as soon as the interaction between the tributary flows started. The direction of the velocity vectors in the plan view indicates this flow element. Further downstream and specifically in the last cross section, flow recovery was obtained and spanwise velocity is almost nil. Regarding maximum velocity, it was particularly evident in the region near the channel bottom. the main flow elements that may be identified in symmetric confluence flows. The influence of tributaries discharge, momentum and width ratios on these flow elements is described herein. The interaction of the flows in the two tributaries with an angle close to the angle of the channels leads to the deflection of the flow towards the outer part of the channel wall. Together with this flow deflection, a stagnation area located in the junction between the tributaries is created. The cross-sectional velocity vectors reflected the secondary currents formed in the confluence joint channel. For every flow case, two secondary cells were observed in the first cross section. These cells stand for the two spiral jets with different magnitudes depending on the width and momentum ratio. Features of high width and momentum ratio which leads to higher secondary velocities for tributary. Due to the much higher streamwise velocity from that tributary, especially near water surface, this secondary flow was transported downstream and eventually became the only secondary cells in the cross sections (Leila and Fernandes, 2021).

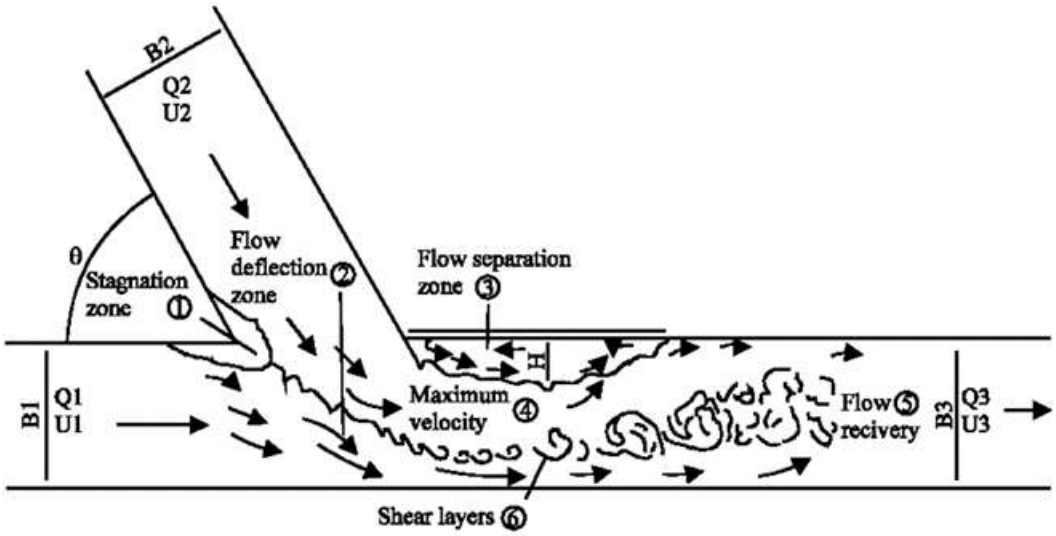


**Figure 1: Flow pattern of Confluence**

As the flows from two tributaries merge and adjust to the confluences planform geometry substantial changes to the flow hydrodynamics and bed morphology occur within and immediately downstream of the

confluence. This region where the local hydrodynamics are influenced by the convergence and realignment of the combining flows at the confluence is known as the Confluence Hydrodynamic Zone. It is generally acknowledged that the hydrodynamics and morpho-dynamics (i.e. patterns of erosion and deposition) within the confluence hydrodynamic zone (CHZ) are influenced by the planform of the confluence; junction angle of confluence ( $\theta$ in Figure 1); momentum flux ratio of merging streams (Mr); and level of concordance between channel beds at the confluence entrance. The fluid dynamics about confluences have a highly complex three-dimensional flow structure which generally includes a zone of flow stagnation near upstream junction corner; an area of flow deflection as tributary flows enter confluence; shear layer and/or mixing interface between the two converging flows; a possible zone of separated flow about the downstream junction corner(s); flow acceleration within the downstream channel; and flow recovery at the downstream end of the CHZ. Of the thousands of natural confluences on Earth, only detailed studies of around one hundred confluences have been presented in peer review publications, with most of these studies concentrating on confluence morpho-dynamic and mixing processes. Large scale hydrodynamics (e.g. depth-averaged velocity patterns) scale reasonably well with large variations in confluence size. However one noticeable region of difference between flume and natural confluences dynamics seems to be within the downstream region of the CHZ where the magnitude of velocity difference across the mixing interface, the length of flow recovery and mixing length seem to differ, with these generally seeming smaller in flume studies. Another example of this possible discrepancy relates to the separation zone about the junction corner observed. Such downstream separation regions have rarely been reported during past field experiments in smaller natural confluences. For the discharge ratio (q = Q1/Q2) and junction angle ( $\theta$ ). Velocity fluctuations about the mean flow velocity by long period oscillations and large macro-turbulence (Mark *et al.*, 2015) seemed to cause the lateral roll over of the mixing interface instability waves (e.g. Kelvin-Helmholtz) creating large vortices of waters and subsequent lateral bursting of these vortices towards one side. Therefore it is important to study the influence of long-period oscillations and the interaction of the flow with the local bathymetry to better understand the hydrodynamics about large confluences.

Mid-channel bars and their associated confluences are key morpho-dynamic nodes within braided rivers, with past studies having investigated the morpho-dynamics of small natural channels or laboratory models with relatively low width/depth (W/D) ratios, typically at W/D <10. The morphology, suspended bed sediment distribution, and flow structure at two large braid bar confluences wherein W/D ratios are much higher (approaching 100) than in smaller channels. The results highlight the significant control of the cross-sectional distribution of downstream flow velocity on confluence flow, suspended bed sediment concentration, and morpho-dynamics and indicate that this factor may become progressively more significant with increasing channel scale and W/D ratio, particularly when simple discharge (or momentum) ratios between the incoming flows are used to explain the flow dynamics. Additionally, secondary flow cells, often proposed to occupy a large part of the channel width in small river channel confluences, are only identified in relatively small portions of the channel width at these larger spatial scales. The position of the scour hole appears dependent on the flow momentum ratio between the two confluent rivers, supporting previous field and experimental results in small junctions. However, the discharge ratio Q1/Q2 may not be the most important variable controlling the position and dimensions of the scour hole, since the actual location and distribution of the cores of primary velocity across the large widths of the confluent channels may have the most significant influence. Bed discordance between the confluent branches is present at both junctions but they do not form true "avalanche faces." The flanks of the scours are very low angle and are incapable of generating regions of permanent flow separation as observed at many smaller confluences with lower W/D ratios. Secondary circulation, although present, is restricted to less than 20 % of the channel width, unlike those cells measured at smaller confluences where the width of such cells may extend up to 50 –80 % of the channel width. Moreover, this restriction of secondary circulation seems related to the generative mechanisms of secondary flows at these higher W/D ratios, which are found to be dominated by

shear-induced turbulence and concentrated close to the mixing interface over the scour region (Ricardo *et al.*, 2009).

Confluence–diffluence units are key elements within many river networks, having a major impact upon the routing of flow and sediment, and hence upon channel change. Although much progress has been made in understanding river confluences, and increasing attention is being paid to bifurcations and the important role of bifurcation asymmetry, most studies have been conducted in laboratory flumes or within small rivers with width/depth (aspect) ratios less than 50. This paper presents results of a field-based study that details the bed morphology and 3D flow structure within a very large confluence–diffluence in the Río Paraná, Argentina, with a width/depth ratio of approximately 200. Flow within the confluence–diffluence is dominated largely by the bed roughness, in the form of sand dunes; coherent, channel-scale, secondary flow cells, which have been identified as important aspects of the flow field within smaller channels, and assumed to be present within large rivers, are generally absent in this reach. This finding has profound implications for flow mixing rates, sediment transport rates and pathways, and thus the interpretation of confluence–diffluence morphology and sedimentology. Secondary currents are generally classified into two main types: those generated by interactions between centrifugal and pressure gradient forces and those produced by the heterogeneity and anisotropy of turbulence. Two issues arise in defining such secondary currents: (1) definition of a suitable frame of reference and (2) correct interpretation of the differences between permanent and turbulence-driven secondary flows. The secondary flows along each cross-sectional transect were calculated using the Rozovskii method, which involves depth-integrating each velocity profile in the section to obtain the depth averaged velocity vector. The differences from this depth-averaged velocity for all measurements within the profile are then computed to provide an indication of secondary motions in the plane perpendicular to the average velocity direction in the profile. Although the Rozovskii method for determination of secondary currents is problematic, it was chosen herein since, if there is any type of secondary circulation present, this rotation method will identify it. The calculated secondary flow vectors superimposed on the downstream flow contours at three sections through the confluence–diffluence unit. The absence of secondary circulation may appear surprising: the channels are curved with significant convergence and divergence, and it may be expected that flow direction at the surface would differ from that at the bed, as the latter is more strongly steered by bed topography. The fact that there is a near uniform flow direction throughout the flow depth suggests that the steering of flow at the bed is readily transmitted throughout the flow depth, preventing channel-scale differences between near-bed and near-surface flow

directions. Figure 6 shows the vertical velocities in the left channel at the diffluence section and indicates a strong correlation between zones of down-welling flow and the positions of the dune lee sides, with fluid upwelling being associated with the dune stoss sides. These dunes appear to scale approximately with the flow depth, with dune heights approaching 2·2 m, similar to those found in past studies. Thus, although the flow depth in these large rivers is obviously greater than in smaller rivers, which should encourage greater divergence between near-bed and near-surface flows, the fact that the dune roughness scales with the flow depth allows the effects of the bed topography to be transmitted through the flow depth, therefore assisting with the steering of flow throughout the vertical. The flow field within the confluence–diffluence unit is dominated by simple convergence and divergence through this nodal area, and at this flow stage and discharge ratio no coherent, channel-scale secondary flow cells appear to exist at the confluence as has been proposed from smaller rivers. Although there is a suggestion of one, full-width, cell over the central scour, there is no evidence of coherent secondary cells as flow shallows at the diffluence. It is evident that at these flow levels in this very wide river, flow mixing and secondary flows are almost completely dominated by bedform roughness. As a result, the coherent secondary flow cells that have been identified in smaller channels, and often assumed to be present within large rivers, are generally absent through this large confluence–diffluence unit (Daniel *et al.*, 2006).

*International Journal of Applied Engineering and Technology ISSN: 2277-212X*
*An Open Access, Online International Journal Available at http://www.cibtech.org/jet.htm*
*2022, Vol.12, pp.12-22/Edward*
***Research Article***

## EXAMPLES OF THE EXPLANATIONS AND SOLUTIONS OF CONFLUENCE AND DEFLUENCE FLOW WITH VECTORS

### *A. The Vector Concepts:*

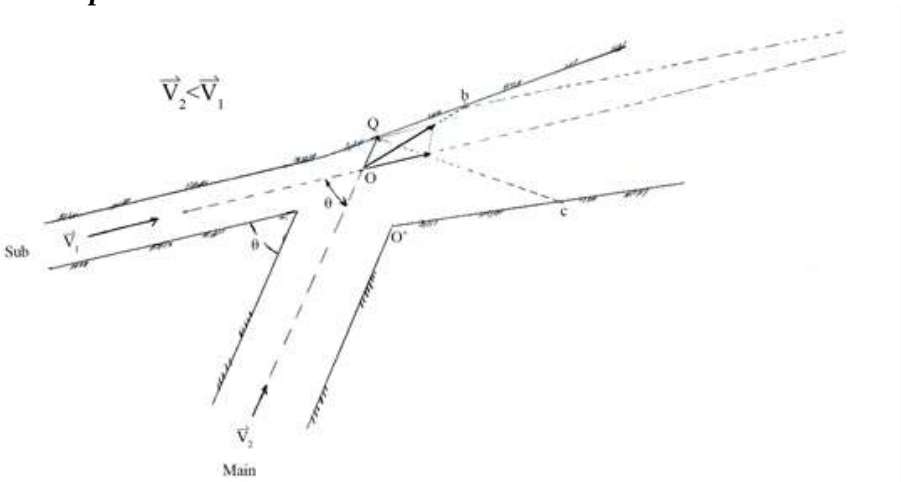


**Figure 2: (1) Confluence Flow: the stronger velocity in sub-channel**

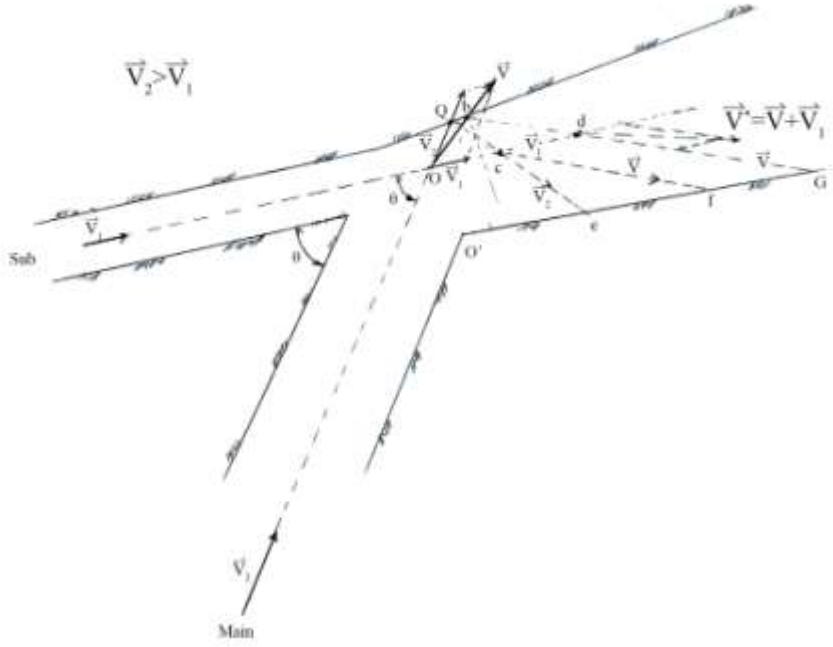


**Figure 2: (2) Confluence Flow: the stronger velocity in main-channel**

The angle $\theta$ and the vector of the velocity for the stronger one are both the important factors to determine the flow pattern on confluence and the sediment transport of deposition region. The flow situation in Fig. 2. (2) is much more complicated the deposition zone will extend from point $O'$ to point G and the velocity change diversifying than the ones of Fig. 2. (1).

And how will be the situations if the positions of main channel and sub-channel change each other? In the following two figures, the phenomena present us that the stronger velocity has the small intersecting angle with the flow direction of confluence flow, the smooth flow condition is shown, otherwise, varying one happens. The results are as follows:

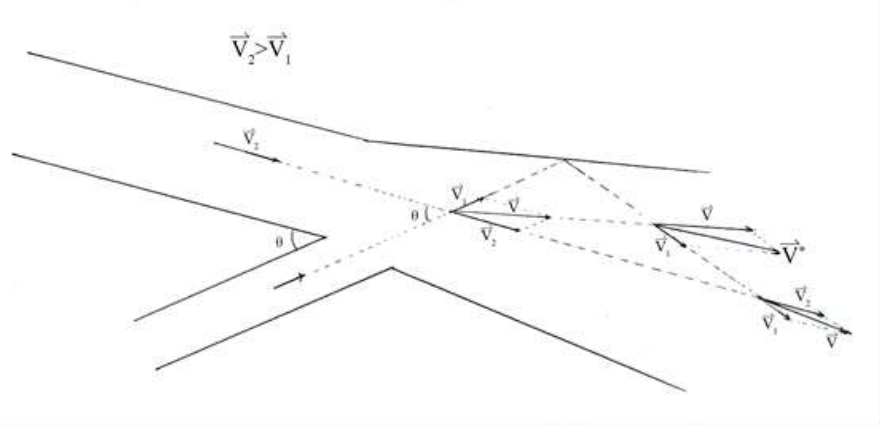


**Figure 3 (1): Confluence Flow: the stronger velocity in main-channel**

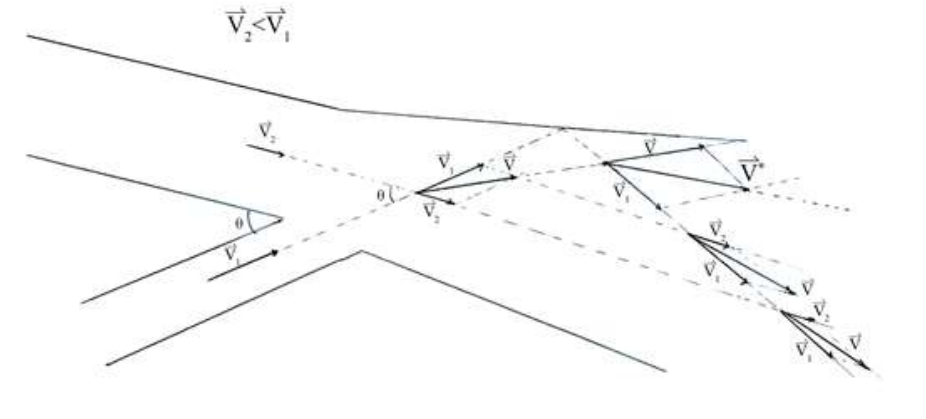


**Figure 3(2): Confluence Flow: the stronger velocity in sub-channel**

***B. Two Examples with the Calculations for Confluence and Diffluence Respectively***

**1. Confluence**

For the given values of inflow discharges of $Q_1$and $Q_2$ with the relatively bed slopes $s_1$and $s_2$,the angles before combination, $\theta_1$and $\theta_2$ with the flow velocity after combination, V, the 1D flow analysis has been done as follows:

$Q_1+Q_2= Q$……..….....(9)

$\vec{M}$=ρ$Q\vec{V}$ $\overrightarrow{M_1}$=ρ$Q_1\overrightarrow{V_1}$ $\overrightarrow{M_2}$=ρ$Q_2\overrightarrow{V_2}$

ω=ρ$Q$s $\omega_1$=ρ$Q_1s_1$ $\omega_2$=ρ$Q_2s_2$

Then $M_x$=ρ$QV$ = ρ$Q_1V_1$cos$\theta_1$+ρ$Q_2V_2$cos$\theta_2$……..…...……..…….....(10)

$M_y$=0=ρ$Q_1V_1$sin$\theta_1$-ρ$Q_2V_2$sin$\theta_2$…….....(11)

ω=ρ$Q$s=$\omega_1 + \omega_2$ = ρ$Q_1s_1$ + ρ$Q_2s_2$……...….(12)

From Eq.(12) $\frac{Q}{Q_1} = s_1$/s+r$s_2$/s with $\frac{Q_2}{Q_1} = r$

From Eq.(10) $\frac{Q}{Q_1}V = V_1$cos$\theta_1$+r$V_2$cos$\theta_2$……..…...(13)

From Eq.(11) $\frac{Q_2}{Q_1} = r$ =($V_1/V_2$)(sin$\theta_1$/sin$\theta_2$)

$\frac{V_2}{V_1}$ =k/r with (sin$\theta_1$/sin$\theta_2$) = $r$…….....(14)

Substituting Eq. (14) into Eq. (13) we have:

$V_1 = \frac{QV}{NQ_1} = (\frac{V}{N})(s_1$/s+r$s_2$/s)…….…….....(15)

With Eq.(12) and N=$\cos\theta_1 + k\cos\theta_2$ and $V_2$ =(k/r) $V_1$in Eq.(14)

**2. Diffluence:**

For the given values of inflow discharges of $Q$ and V with the relatively bed slopes s, $s_1$and $s_2$, and the angles after defluence, $\theta_1$and $\theta_2$ , the 1D flow analysis has been done as follows:

$Q_1$+$Q_2$= $Q$……..…….....(16)

$\vec{M}$=ρ$Q\vec{V}$ $\overrightarrow{M_1}$=ρ$Q_1\overrightarrow{V_1}$ $\overrightarrow{M_2}$=ρ$Q_2\overrightarrow{V_2}$

ω=ρ$Q$s $\omega_1$=ρ$Q_1s_1$ $\omega_2$=ρ$Q_2s_2$

Then $M_x$=ρ$QV$ = ρ$Q_1V_1\cos\theta_1$+ρ$Q_2V_2\cos\theta_2$……..……...……....……..(17)

$M_y$=0=ρ$Q_1V_1\sin\theta_1$-ρ$Q_2V_2\sin\theta_2$……..……..(18)

ω=ρ$Q$s=$\omega_1 + \omega_2$ = ρ$Q_1s_1$ + ρ$Q_2s_2$……..…..……(19)

From Eq.(4) $\frac{Q}{Q_1} = s_1/s+rs_2/s$ with $\frac{Q_2}{Q_1} = r$

From Eq.(17) $\frac{Q}{Q_1}V = V_1\cos\theta_1$+r$V_2\cos\theta_2$……..…..……..……..…(20)

From Eq.(18) $\frac{Q_2}{Q_1} = r = (V_1/V_2)(\sin\theta_1/\sin\theta_2)$

$\frac{V_2}{V_1}$ =k/r with $(\sin\theta_1/\sin\theta_2) = r$…….....(21)

Substituting Eq. (21) into Eq. (20) we have:

$V_1 = \frac{QV}{NQ_1} = (\frac{V}{N})(s_1/s+rs_2/s)$……..……..…....(22)

With Eq.(19) and N=$\cos\theta_1 + k\cos\theta_2$ and $V_2$ =(k/r) $V_1$in Eq.(21). For a given r , $V_1$ and $Q_1$ can be obtained from Eq. (22), $Q_2$ from Eq.(1) and $V_2$ from Eq. (18)..

## CONCLUSIONS

### *1. Velocity Variation*

Flow separation in the post-confluence channel causes streamlines to be contracted and creates a contraction zone. Flow contraction and also combination of the main and the tributary channel flows, increase water velocity in this zone. It can be seen that the maximum velocity Umax occurs in the contraction zone. It is important to identify the location and magnitude of the maximum velocity because maximum shear stress and therefore scouring are expected to appear in this location. The effect of flow controllers on non-dimensional maximum velocity, Umax/Ud (Ud the downstream flow velocity). As mentioned, the higher the discharge ratios, the smaller the separation zone leads to less flow contraction and reduction in Umax. Under these circumstances, non-dimensional maximum velocity approaches to unity. However, for smaller confluence angles, Umax/Ud does not show much sensitivity to discharge ratio. In channels with small angles, where the main and the tributary channels approach the post confluence channel approximately in the same direction, flow contraction is not significant, while the contraction zone becomes narrower and its velocity is increased by an increase in the confluence angle because of more expansion in the separation zone. Where the tributary channel width is less than that of the main channel, flow velocity in the tributary channel is increased under the constant discharge. As a result, dimensions of the separation zone expand, thus leading to more flow contraction and rise in the maximum flow velocity. The flow velocity increases in both the contraction zone and the downstream section of post-confluence, when Fd (Froude number) increases; therefore, Fd variations do not have considerable effect on the ratio of Umax to Ud.

### *2. Surface Variations*

Two significant factors may explain water surface variations. Firstly, radial pressure gradient, induced by tributary flow deflection in the main channel, causes a sharp water surface drawdown in the center of deflection at the downstream corner of the confluence and water surface afflux at the upstream corner of

confluence and beyond the deflection flow line. Secondly, flow contraction at the confluence causes water surface drawdown in this zone. The minimum and maximum water surface elevations in the whole confluence, Zmin and Zmax, are considered as two main elements of water surface in the confluence; Zmin occurs in the downstream corner of the confluence, where the separation zone initiates, while Zmax occurs in the main channel and (or) beginning of the tributary. The less the discharge ratios, the more the tributary channel deflection and the flow contraction. These changes result in decrease and increase of Zmin and Zmax. The maximum and the minimum water surface elevations Zmax and Zmin, increase and decrease when the confluence angles are higher. For small angles, the difference between Zmax and Zmin is insignificant and is less than 5% of the downstream water depth. The effect of width ratio on water surface variations is considerable only at low discharge ratios. Increasing Froude number of downstream leads to more flow deflection as well as contraction that causes an increase in Zmax and a decrease in Zmin.

### *3. Secondary Currents and Vortex*

Flow structure at channel confluences is highly affected by a complex vortex system. The tributary channel flow, at the entrance of the confluence, detaches from the inner wall and attaches again at the downstream section and creates a separation zone with a rotational flow. Flow separation causes combined flow to be contracted and creates a contraction zone at which maximum velocity takes place. Flow deflection leads to water surface drawdown at the downstream corner and afflux in the upstream channels. In addition, this deflection generates a strong helical cell in the post-confluence channel, besides interaction of the strong tributary helical cell and the main flow creates a third weaker helical cell, which rotates in a direction opposite to the tributary helical cell. The results illustrate that an increase in the confluence angle and Froude number as well as a decrease in discharge and width ratios leads to a larger separation zone, a narrower contraction zone with the higher velocity, stronger and more distinguishable helical cells, and also intensified water surface variations in the confluence. Various graphs are presented for dimensions of the separation zone and water surface rise and drawdown on the basis of the numerical model results.

## REFERENCES

**Axtmann EV, Cain, DJ and Luoma SN (1997).** Effect of tributary inflows on the distribution of trace metals in fine-grained bed sediments and benthic insects of the Clark Fork river, *Montana. Environment Science and Technology*, 31, 750–758.

**Bernard De Serres, Andre G. Roy, Pascale M. Biron, James L. Best, (1999).** Three-dimensional structure of flow at a confluence of river channels with discordant beds, *Geomorphology*, 26, 313–335.

**Best JL, Roy AG (1991).** Mixing-layer distortion at the confluence of channels of different depth. *Nature* 350, 411–413.

**Biron P, Best JL, Roy AG (1996a)**. Effects of bed discordance on flow dynamics at open channel confluences. *Journal of Hydraulic Engineering ASCE* 122, 676–682.

**Biron P, Roy AG, Best JL (1996b)**. Turbulent flow structure at concordant and discordant open-channel confluences. *Experiments in Fluids*, 21, 437–446.

**Bradbrook KF, Lane SN, Richards KS, Biron PM and Roy AG (2001)**. Role of bed discordance at asymmetrical river confluences. .*Journal of Hydraulic Engineering*, 127 351-368.

**Daniel R Parsons, James L Best, Stuart N Lane, Oscar Orfeo, Richard J Hardy, and Ray Kostaschuk (2007).** Form roughness and the absence of secondary flow in a large confluence–diffluence, Rio Paraná, Argentina. Earth Surface Processes and Landforms Earth Surf. Process. Landforms 32, 155–162 (2007) Published online 13 November 2006 in Wiley InterScience (www.interscience.wiley.com) DOI: 10.1002/esp.1457

**Gaudet JM, Roy AG (1995).** Effect of bed morphology on flow mixing length at river confluences. *Nature* 373, 138–139

**Kennedy BA (1984)**. On Playfair's law of accordant junctions. *Earth Surface*. Processes Landforms 9, 153–173.

**Leila Alizadeh and João Fernandes (2021).** Turbulent flow structure in a confluence: influence of

tributaries width and discharge ratios. *Water* 2021, 13, 465. *https://doi.org/10.3390/w13040465.*
**Mark Trevethan, Ander Martinelli, Marco Oliveira, Marco Ianniruberto & Carlo Gualtieri (2015).** FluidL mechanics, sediment transport and mixing about the confluence of NEGRO and SOLIMÕES rivers, MANAUS, BRAZIL. *E-proceedings of the 36th IAHR World Congress* 28 June – 3 July, 2015, The Hague, the Netherlands.
**Ricardo N Szupiany, Mario L Amsler, Daniel R Parsons and James L Best (2009).** Morphology, flow structure, and suspended bed sediment transport at two large braid-bar confluence. *Water Resources Research*, 45, W05415, doi:10.1029/2008WR007428, 2009.